International Journal of Pharmaceutics 400 (2010) 201–210

Contents lists available at ScienceDirect

International Journal of Pharmaceutics

journal homepage: www.elsevier.com/locate/ijpharm

Pharmaceutical Nanotechnology

Wheat germ agglutinin-conjugated PLGA nanoparticles for enhanced intracellular delivery of paclitaxel to colon cancer cells

Chunxia Wang[a], Paul C. Ho[a], Lee Yong Lim[b,*]

[a] Department of Pharmacy, National University of Singapore, 18 Science Drive 4, Singapore 117543, Singapore
[b] Pharmacy M315, School of Biomedical, Biomolecular and Chemical Sciences, University of Western Australia, 35 Stirling Highway, Crawley, WA 6009, Australia

ARTICLE INFO

Article history:
Received 6 May 2010
Received in revised form 5 August 2010
Accepted 22 August 2010
Available online 8 September 2010

Keywords:
Wheat germ agglutinin (WGA)
Paclitaxel
PLGA nanoparticles
Colon cancer
Intracellular delivery

ABSTRACT

The purpose of this study was to investigate the potentiation of the anticancer activity and enhanced cellular retention of paclitaxel-loaded PLGA nanoparticles after surface conjugation with wheat germ agglutinin (WGA) against colon cancer cells. Glycosylation patterns of representative colon cancer cells confirmed the higher expression levels of WGA-binding glycoproteins in the Caco-2 and HT-29 cells, than in the CCD-18Co cells. Cellular uptake and *in vitro* cytotoxicity of WNP (final formulation) against colon cell lines was evaluated alongside control formulations. Confocal microscopy and quantitative analysis of intracellular paclitaxel were used to monitor the endocytosis and retention of nanoparticles inside the cells. WNP showed enhanced anti-proliferative activity against Caco-2 and HT-29 cells compared to corresponding nanoparticles without WGA conjugation (PNP). The greater efficacy of WNP was associated with higher cellular uptake and sustained intracellular retention of paclitaxel, which in turn was attributed to the over-expression of N-acetyl-D-glucosamine-containing glycoprotein on the colon cell membrane. WNP also demonstrated increased intracellular retention in the Caco-2 (30% of uptake) and HT-29 (40% of uptake) cells, following post-uptake incubation with fresh medium, compared to the unconjugated PNP nanoparticles (18% in Caco-2) and (27% in HT-29), respectively. Cellular trafficking study of WNP showed endocytosed WNP could successful escape from the endo-lysosome compartment and release into the cytosol with increasing incubation time. It may be concluded that WNP has the potential to be applied as a targeted delivery platform for paclitaxel in the treatment of colon cancer.

1. Introduction

The ideal goal of cancer chemotherapy is to destroy cancer cells without harming healthy cells. Most anticancer drugs fall short of this ideal. Drugs that are not specific in action accumulate not only in the tumor cells but also in the healthy tissues, causing significant morbidity and mortality. In the case of colon cancer, the intravenous delivery of anticancer agents often causes severe side-effects (De Dosso et al., 2009; Holt et al., 2009). To overcome this drawback, significant efforts have been made to develop appropriate targeting systems for colon-specific drug delivery (Casadei et al., 2008; Patel et al., 2007; Yang, 2008). Among the systems developed, nanotechnology-based platforms appear promising in improving therapeutic outcome by focusing drug delivery to the target site, and minimizing drug accumulation at non-specific sites (van Vlerken et al., 2007). Of the nanoparticulate systems reported in the literature, PLGA nanoparticles are versatile because they offer a biocompatible vehicle that also present opportunities for drug targeting at the cellular level (Mohamed and van der Walle, 2008). PLGA nanoparticles can provide sustained drug release and a surface amendable to chemical conjugation for targeting purposes, and they may bypass the efflux activity of membrane transporters (Chen et al., 2008; Keegan et al., 2006; Panyam and Labhasetwar, 2003; Sahoo and Labhasetwar, 2003).

Paclitaxel is one of the most effective anticancer agents available clinically. It has a wide spectrum of activity against solid tumors, including colon cancer (Huh et al., 2009; Suffness and Wall, 1995; Zhan et al., 2009). Its clinical application is, however, limited by an intractable insolubility in aqueous media and a non-specific activity against both cancerous and normal cells. The clinical formulation is Taxol®, which comprises a 1:1 v/v mixture of Cremophor EL® and ethanol as vehicle (Singla et al., 2002). Several studies have shown Cremophor EL to be a problematic vehicle (Trissel, 1996; Trissel et al., 1994). The incorporation of paclitaxel into PLGA nanoparticles was promising in resolving the aqueous solubility of the drug. However, cellular uptake of PLGA nanoparticles is of low capacity (Chen and Langer, 1998) and specificity (Kim and Nie, 2005). For some drugs, whose targets are in the cytoplasmic or other intracellular compartments, such as the nucleus or mitochondria, it is necessary for the drug to be delivered to these specific locations in

* Corresponding author. Tel.: +61 8 64884413; fax: +61 8 64881025.
E-mail address: limly@cyllene.uwa.edu.au (L.Y. Lim).

0378-5173/$ – see front matter © 2010 Elsevier B.V. All rights reserved.
doi:10.1016/j.ijpharm.2010.08.023

order for it to exert its pharmacological effect. Such as the case for paclitaxel, whose anticancer activity is realized by its effective binding to the intracellular microtubules (Andreopoulou and Muggia, 2008). In addition to a targeted drug disposition, the duration of drug retention at the target site could be critical to achieve the desired therapeutic outcome in cancer treatment. Cancer is a disease condition that requires prolonged drug exposure to ensure complete regression of the tumor and avoidance of a relapse (Jang et al., 2003). To improve the efficiency of PLGA nanoparticles as a carrier for intracellular paclitaxel delivery, we functionalized the nanoparticle surface with wheat germ agglutinin in order to promote their internalization and sustained retention by the target cells (Mo and Lim, 2005a,b). Previous experiments in our laboratory have shown that the conjugation of WGA to PLGA nanoparticles loaded with paclitaxel could improve the intracellular delivery of paclitaxel to small lung cancer cells relative to lung fibroblasts (Mo and Lim, 2005a,b).

WGA is present at approximately 300 mg/kg in wheat flour (Pusztai et al., 1993). It is a 36-kDa protein consisting of two identical subunits, with each subunit comprising an assembly of four homologous domains (Lehr, 2000). WGA can specifically recognize and bind rapidly with N-acetylglucosamine and sialic acid residues on cell membrane, which leads to cellular internalization through receptor-mediated endocytosis (Caldero et al., 1989). A histochemical study using lectin has shown that WGA can bind to colon tissue. Compared with plant lectins of different carbohydrate specificity, e.g. peanut agglutinin (PNA), WGA has the highest binding rate to colonic carcinomas of human origin, normal mucosa and human colonocytes (Caldero et al., 1989; Campo et al., 1988a; Heinrich et al., 2005). WGA therefore has the potential to be a good ligand for the targeted delivery of anticancer drugs to the colon (Minko, 2004). However, WGA related glycosylation pattern of colon cancer and normal cells is not very well characterized. Moreover, few past studies have tested the WGA-conjugated PLGA nanoparticles on both cancer and non-cancer cells of colon.

Our objective was to exploit the cytoadhesive and cytoinvasive properties of WGA to develop a colon cancer targeted PLGA nanoparticulate system for paclitaxel. For this reason, it was proposed that the conjugation of WGA to PLGA nanoparticles loaded with paclitaxel (WNP) could improve the delivery of paclitaxel to colonic cancer cells. To evaluate the differential uptake and efficacy of WNP in appropriate colon cell models, WNP nanoparticles were prepared according to the method developed in our laboratory (Mo and Lim, 2005a). Cellular uptake of WNP by the colon cancer cell lines, Caco-2 and HT-29, and the colon fibroblast cell line, CCD-18Co, was quantified by a fluorometric method through the use of FITC-labelled WGA (fWGA) to prepare the nanoparticles. The uptake data were correlated with cytotoxicity data for both the test formulation and control formulations against the colon cell lines. In addition, the intracellular translocation of WNP in the Caco-2 cells was monitored as a function of time. WGA-conjugated, paclitaxel-loaded PLGA nanoparticles are designated as WNP, while the corresponding fWGA-conjugated nanoparticles are designated as fWNP. Control formulations consisted of (a) paclitaxel-loaded PLGA nanoparticles without WGA conjugation (PNP), (b) equivalent Taxol® formulation of paclitaxel dissolved in a 1:1 v/v solvent mixture of Cremophor EL and ethanol at 6 mg/ml (P/CreEL), and (c) drug-free nanoparticles conjugated with WGA (WN), fWGA (fWN) and FITC-labelled BSA (fBSA) conjugated nanoparticles (fBN).

2. Materials and methods

2.1. Materials

Resomer® RG 502H (PLGA, lactide:glycolide = 50:50, acid number of 10.7 mg KOH/g) was a product of Boehringer Ingelheim, Germany. Wheat germ agglutinin (WGA), FITC-labelled wheat germ agglutinin (fWGA, FITC content 2.5 mol/mol lectin), FITC-labelled BSA (fBSA, FITC content 12 mol/mol BSA), 1-ethyl-3-(3-dimethylaminopropyl)carbodiimide hydrochloride (EDAC), N-hydroxysuccinimide (NHS), polyvinyl alcohol (PVA, mw 30,000–70,000), propidium iodide (PI), isopropyl myristate (IPM), trypsin/EDTA (10×), 3-(4,5-dimethylthiazolyl-2)-2,5-diphenyl tetrazolium bromide (MTT), Eagle's MEM and trypan blue were products of the Sigma Chemical Co. (St. Louis, MO, USA). Biotinylated-wheat germ agglutinin and Vectastain Elite ABC kit were from Vector Laboratory (Burlingame, CA, USA); protease inhibitor was from Roche Diagnosis (Basel, Switzerland); The Micro BCA protein assay kit was from Pierce Biotechnology Inc (Rockford, IL, USA). Paclitaxel (microcrystalline powder, >99.5% purity) was purchased from the 21CEC Company (Oaklands, UK) while Lysotracker red DND-99, Hoechst 33342, MEM and McCoy 5A were from Invitrogen (Grand island, NY, USA). Caco-2 cells (human, male colon cancer cell line) were purchased from the Riken Bioresource Center (Koyadai, Tsukuba, Ibaraki, Japan). HT-29 cells (human, female colon cancer cell line) and CCD-18Co cells (human colon fibroblast) were purchased from the American Type Culture Collection (VA, USA).

2.2. Methods

2.2.1. Cell culture

Caco-2 cells were cultured in MEM supplemented with 10% FBS, 1% NEAA, 1% penicillin and 1% streptomycin. HT-29 and CCD-18Co cells were cultured in McCoy's 5A and Eagle's MEM, respectively, both of which were supplemented with 10% foetal calf serum, 1% penicillin and 1% streptomycin. Cell cultures were incubated at 37 °C in a humidified atmosphere of 5% CO_2 and 95% air (NuAire US autoflow, NuAire Inc., MN, USA), with medium exchange on alternate days. Cell viability (>98%) was assessed by diluting the cell suspension with an equal volume of 0.4% trypan blue solution and counting the cells using a hemacytometer (Tiefe, Germany).

2.2.2. Protein extraction and lectin blot analysis

For total cell protein extraction, cells were cultured on 25 cm^2 flasks for 3 days. Confluent cells after washing thrice with ice-cold PBS were suspended in PBS with a cell scraper. Cell suspension was transferred into 1.5 ml-eppendorf tubes and centrifuged at 3000 × *g* for 2 min at 4 °C (MIKRO 22R, Andreas Hettich GmbH & Co KG, Tuttlingen, Germany). The supernatant was discarded and the cell pellet was resuspended in lysis buffer (PBS containing 1% of Triton X-100 and protease inhibitor). After 30 min incubation on ice with occasional vortex, the cell lysate was centrifuged at 10,000 × *g* at 4 °C for 20 min, and aliquots of the supernatant were stored at −80 °C till further use.

Cell membrane protein was extracted according to the manufacturer's instructions for the Mem-PER eukaryotic membrane protein extraction reagent kit (Pierce Biotechnology, Rockford, IL, USA). The extraction method required cell lysis with a detergent, and a second detergent was added to solubilize the membrane proteins. After a quick centrifugation, the cocktail was incubated at 37 °C to separate the hydrophobic membrane proteins from the hydrophilic proteins through phase partitioning. The hydrophilic proteins were assumed to be the intracellular proteins excluding the cell membrane protein. The membrane proteins were stored at −80 °C until analysis.

Protein was quantified using the Micro BCA protein assay according to the manufacturer's instructions. Protein samples equivalent to 5 μg of protein were size-fractionated on a 7.5% SDS-PAGE (Mini-PROTEAN 3 System, Bio-Rad Laboratories, Hercules, CA, USA) at 150 V for 1.5 h, and transferred to PVDF membranes, which were blocked by overnight incubation in a buffer (TBST)

containing 1% of Tween 20, 200 mM of NaCl and 50 mM of Tris. The membranes were probed with biotinylated WGA for 1 h. After washing (3 × 10 min), the membranes were incubated for 1 h at room temperature with the avidin–biotin-peroxidase solution from the Vectastain reagent kit. The glycoprotein was detected using the west pico chemiluminescence system. Bands were visualized in a CCD imaging machine (Fluorchem® HD2, Alpha Innotech, San Leandro, CA, USA).

2.2.3. Preparation of WGA-conjugated, paclitaxel-loaded PLGA nanoparticles

PLGA nanoparticles with and without the incorporation of paclitaxel were manufactured by a modified emulsion solvent evaporation method (MESE) according to the method developed in our laboratory (Mo and Lim, 2005b). In brief, PLGA (100 mg), IPM (30 mg) and, if required, paclitaxel (10 mg), were dissolved in 5 ml of methylene chloride. The organic phase was emulsified in 50 ml of aqueous surfactant solution (0.5% w/v of PVA) by probe sonication (Sonics VC-130, Sonics and Materials Inc., CT, USA, 25 W output, 2 min, pulse 2 s) on an ice bath, and further magnetically agitated at 1000 rpm (Thermolyne, IA, USA) for 5 h to completely remove the organic solvent.

WGA was conjugated to the surface of the PLGA nanoparticles by a two-step EDAC method. This method involves the activation of the free carboxyl groups on the particle surface in an EDAC/NHS aqueous mixture, followed by conjugation of the activated groups with the amino groups in the WGA molecules. To conjugate the surface of the PLGA nanoparticles with WGA, the nanoparticles dispersion was mixed with 1 ml of 0.1 M EDAC/0.7 M NHS at 100 rpm for 1 h at room temperature. Excess reaction medium was removed by crossflow filtration. The nanoparticles were then incubated with 2 ml of WGA (1 mg/ml in PBS) overnight and unreacted WGA was separated from the nanoparticles by crossflow filtration. Excess coupling sites were blocked by glycine. Preparation of corresponding fWGA- and fBSA-conjugated PLGA nanoparticles followed similar procedures except that equivalent concentrations of fWGA and fBSA were used in place of WGA.

2.2.4. Characterization of nanoparticles

Nanoparticles were characterized for particle size and zeta-potential by a particle size analyzer (Zetasizer 3000HSA, Malvern Instruments Ltd., Worcestershire, England). The morphology of the nanoparticles was observed under a transmission electron microscope (TEM, Jeol Electron Microscope, JEM-100CXII, Japan) and a scanning electron microscope (SEM, Hitachi S-4200, Japan). Efficiency of WGA conjugation and paclitaxel loading were determined according to a method described by Mo and Lim (2005b). The HPLC method was developed and validated for the quantitation of paclitaxel. Chromatographic separation was achieved on an Agilent 1100 system (Agilent Technologies, Palo Alto, CA) equipped with a C_{18} column (200 mm × 4.6 mm, 5 μm) (Waters, Milford, MA) preceded by a guard column (Waters). Flow rate of 1 ml/min was applied, with UV detection at 229 nm. The mobile phase consisted of 1:1 v/v acetonitrile and water. A linear standard curve was obtained over the concentration range of 0.1–10 μg/ml ($R^2 > 0.99$). Drug loading efficiency was calculated as the weight of paclitaxel relative to the weight of nanoparticles recovered following the lyophilization of the nanoparticles.

2.2.5. Uptake of blank fWGA (fWN)- and fBSA (fBN)-conjugated PLGA nanoparticles

To quantify the uptake of fWN and fBN by the three cell lines, the respective cells were seeded onto 24-well plates at a density of 1.0×10^5 cells/well. Confluent cells were washed and pre-incubated with 200 μl of HBSS/HEPES for 1 h at 37 °C, then incubated for 0.5–3 h at 37 °C with 0.4 ml of the respective nanoparticle dispersion (0.625, 1.25, 2.5, 3.33 or 5.0 mg/ml in HBSS/HEPES). Uptake was terminated by washing the cell monolayers twice with HBSS/HEPES and solubilizing the cells with 0.4 ml of 5% SDS in 0.1 M NaOH. Cell-associated fWN and fBN were quantified by analyzing the fluorescence intensity of the cell lysates in the plate reader. The plate reader was calibrated in the following manner. Cultured cells from the respective cell lines were harvested from the 24-well plates and lyzed in 0.1 M NaOH/5% SDS to a final concentration of 5×10^5 cells/ml. Freshly prepared fWN and fBN dispersions were diluted in the cell lysate to give final concentrations ranging from 0.625 to 5.0 mg/ml, and the fluorescence intensity of the standard solutions were measured in the plate reader (Spectra Fluor plate reader, Tecan, Austria).

2.2.6. Anti-proliferative activity of paclitaxel formulations

The MTT assay was used to investigate anti-cytoproliferative activity of WNP and the control formulations. Caco-2, HT-29, and CCD-18Co cells were plated at around 8000 cells per well, cultured for 24 h to allow for attachment and exposed to WNP, PNP and P/CreEL diluted to specified paclitaxel doses (0–40 μg/ml) with the corresponding supplemented culture media. Treatment with serum-supplemented medium was used as a negative control (0% cell death), and treatment with 0.1% SDS was used as a positive control (100% cell death). Experiments were initiated by aspiration of the culture medium in each well, and incubating the cells with 200 μl of sample or control solutions for 24 or 72 h at 37 °C in the CO_2 incubator. The solution in each well was then aspirated and the cells incubated for a further 4 h with 200 μl of MTT solution (1 mg/ml in PBS). Intracellular formazan crystals were extracted into 100 μl of DMSO, and quantified by measuring the absorbance of the cell lysate at 590 nm (Spectra Fluor plate reader, Tecan, Austria) with DMSO as blank ($n = 6$). Cell viability was calculated as a percent based on the absorbance measured relative to the absorbance obtained from cells exposed to the culture medium containing 0.5% DMSO.

2.2.7. Cellular accumulation and efflux of paclitaxel

Caco-2, HT-29 and CCD-18Co cells were seeded onto 12-mm dishes at a density of 2×10^4 cells/cm^2 and used after 3 days of culture in 10 ml of respective culture medium when they had reached confluency. Cellular uptake experiments were initiated by the addition of fresh culture medium containing WNP, PNP or P/CreEL to give a final paclitaxel concentration equivalent to 40 μg/ml. After 2 h incubation at 37 °C, cells were washed thrice with ice-cold PBS, harvested with a rubber scraper, centrifuged at 10,000 × g for 10 min, and the cell pellets were lysed in 300 μl of methanol under sonication followed by centrifugation. Paclitaxel content in the supernatant was determined using a HPLC method described in Section 2.2.4. To estimate the rate of efflux of paclitaxel, subconfluent cells in petri dishes were incubated with 6 ml of WNP, PNP and P/CreEL in culture medium for 2 h as described above. After the test sample was aspirated and the cells were washed thrice with PBS, the cells were incubated with fresh culture medium devoid of drug for another 2 h at 37 °C. The cells were harvested by scraping with a small spatula, and lyzed in methanol and the paclitaxel in the cell lysate was determined by HPLC analysis. Data are expressed as intracellular paclitaxel content (μg) per unit weight (mg) of total cell protein.

2.2.8. Visualization of cell-associated nanoparticles

Uptake experiments of fWNP were performed on cell monolayers cultured in Lab-Tek® 8-well chambers (Nalge Nunc Inc., Denmark, seeding density of 1.0×10^5 cells/cm^2). Cells were incubated with 200 μl of culture medium over 72 h before they were exposed to 100 μl of fWNP (1 mg/ml in HBSS/HEPES) for 1 h. Uptake was terminated by aspiration of the nanoparticle dis-

persion followed by thrice washing with PBS. To differentiate between extracellular and internalized nanoparticles, the cells were incubated post-uptake with 200 μl of trypan blue (TB) solution (0.2 mg/ml in MES, pH 4) for 3 min so that any fluorescence attributed to extracellular fWNP might be quenched (Sahlin et al., 1983; Thiele et al., 2001). Cell monolayer was then fixed with 200 μl of methanol/acetone (1:1 v/v) at 4 °C for 5 min. Cell monolayer was washed with 3 × 0.4 ml of cold PBS and then preserved with mounting medium for analysis (Zeiss, Heidelberg, Germany).

2.2.9. Cellular trafficking of WNP

Uptake experiments were performed on cell monolayers cultured in Lab-Tek® 8-well chambers, and exposure of the cells to 100 μl of fWNP (1 mg/ml in HBSS/HEPES) for 0.5–3 h. Half an hour before the end of a specified incubation period, Lysotracker Red DND-99 was applied at a final concentration of 1 μM to stain the acidic organelles (late endosomes and lysosomes). Uptake was terminated by aspiration of the medium, and the cells were incubated for a further 10 min with 20 μM of Hoechst 33342 to allow for nucleus staining. The cells were washed thrice with ice-cold HBSS/HEPES and fixed with 100 μl of methanol/acetone (1:1 v/v) at 4 °C for 5 min. Serial cell images proceeding from the base of the chamber to the cell monolayer surface (Z-series images) were recorded using the confocal microscope (Zeiss, Heidelberg, Germany), then reconstructed to provide the intracellular distribution of fWNP. To determine whether cellular uptake of WNP was mediated by WGA–receptor interaction, control experiments were performed by exposing the cells to 100 μl of fWGA (2 mg/ml in HBSS/HEPES) for 1 h prior to conducting the WNP uptake experiments.

2.2.10. Statistical analysis

Data are presented as mean ± standard deviation. Differences between mean values were analyzed for significance by one-way ANOVA using the SPSS 10.0 software. P values ≤0.05 were considered significant.

3. Results

3.1. Lectin blot analysis

To evaluate the potential of WGA as a targeting moiety in colonic cancer tissues, a comparative lectin blot analysis was undertaken with the Caco-2, HT-29 and CCD-18Co cells cultured in 25 cm^2 flasks. Significant protein bands confirmed the sensitivity of the analysis in detecting N-acetyl-D-glucosamine-containing glycoproteins in the cell membrane and the intracellular compartment of these cells (Fig. 1). Amongst the three cell lines, the HT-29 cells showed the greatest abundance of WGA-recognizable glycoproteins both in the membrane protein sample (Fig. 1a) and in the intracellular protein sample (Fig. 1b). Most of the WGA-recognizable glycoproteins in Caco-2 and HT-29 cells had molecular weight > 75 kDa, whereas the CCD-18Co cells showed an apparent lack of such large proteins. The ranking order of expression of WGA-recognizable glycoproteins in the three cell lines was HT-29 > Caco-2 > CCD-18Co. The results are consistent with published data on the differential expression of carbohydrate residues in 21 colon cancer specimens relative to normal tissues (Boland et al., 1982; Campo et al., 1988b). Moreover, the adhesion of WGA to Caco-2 and HT-29 cells was blocked by WGA-specific sugar, suggesting that a ligand for WGA was present on the cell surface (Gabor et al., 1998).

The higher expression levels of WGA-binding glycoproteins in the human colon cancer cell lines, Caco-2 and HT-29, relative to the human colon fibroblasts, CCD-18Co, which served as surrogate normal colon cells in this study, suggest that WGA could be applied as a potential targeting ligand for drug delivery to colon tumors. Moreover, the existence of N-acetyl-D-glucosamine proteins in both the cell membrane and the intracellular compartments of the colon cancer cells might not only help the WGA-conjugated nanoparticles be internalized by these cells, but the nanoparticles could be retained for longer within the cells to allow for effective intracellular drug accumulation to lethal levels (Parveen and Sahoo, 2008; Plattner et al., 2009).

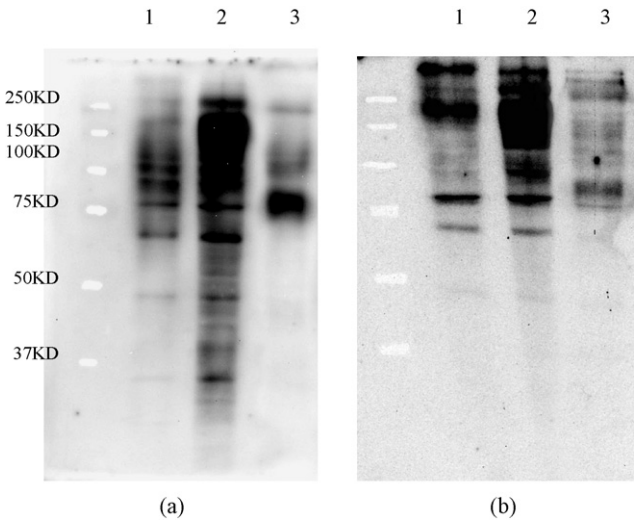

Fig. 1. Lectin blot analysis of (a) cell membrane proteins and (b) intracellular proteins in Caco-2 (lane 1), HT-29 (lane 2) and CCD-18Co (lane 3) cells.

3.2. Characterization of PLGA nanoparticles

As shown previously by our laboratory, and confirmed in this study, the MESE was a simple and reproducible method for the preparation of WGA-conjugated PLGA nanoparticles. The nanoparticles had a particle size of 330 ± 3 nm (n = 3) and polydispersity index of 0.16 ± 0.03 (n = 3). Zeta-potential of nanoparticles was −3.9 ± 0.3 mV (n = 3). The paclitaxel loading efficiency was 53.6 ± 1.8 μg paclitaxel/mg nanoparticles. These results were consistent with previous results obtained by our laboratory (Mo and Lim, 2005b). The WNP nanoparticles had a narrow size distribution, indicating a relatively homogeneous population, and they appeared relatively spherical in shape with no evidence of particle aggregation when viewed under the TEM and SEM (Fig. 2). WGA conjugation efficiency for WNP was 18.1 ± 2.5 μg WGA/mg nanoparticles (n = 3). The collective data suggest that the WNP nanoparticles were reproducible on a batch to batch basis.

3.3. Uptake of fWN and fBN nanoparticles

To determine whether conjugation to PLGA nanoparticles would compromise the capacity of WGA to bind to cell membrane receptors, cellular uptake studies were conducted in the three cell lines using WN nanoparticles prepared with FITC-labelled WGA (fWN). Drug-free PLGA nanoparticles conjugated with FITC-labelled BSA (fBN) served as control. The uptake studies were conducted over incubation time periods ranging from 0.5 to 3 h at nanoparticle loading concentrations of 0.625–5 mg/ml.

As shown in Fig. 3(a) and (c), the Caco-2, HT-29 and CCD-18Co cells showed successful uptake of fWN, indicating that WGA after conjugation to PLGA nanoparticles retained its capacity to recognize and bind to receptors expressed in the cell membranes. Uptake of fWN by the Caco-2, HT-29 and CCD-18Co cells at 0.5 h was 0.57, 0.50 and 0.26 mg NP/mg protein, respectively. The uptake

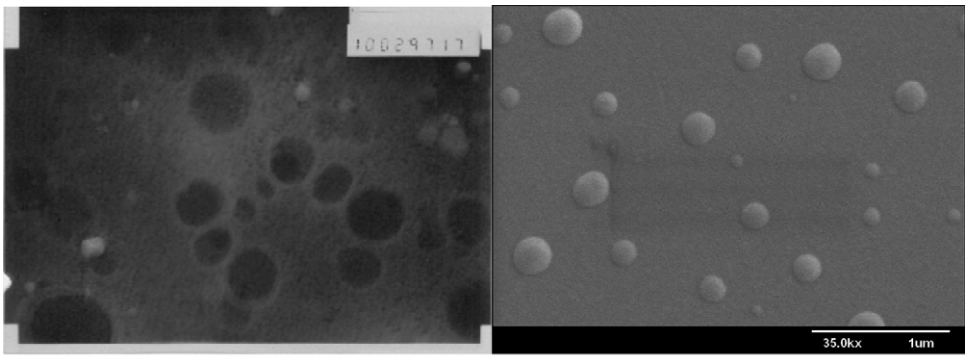

Fig. 2. (a) TEM (magnification 100,000×) and (b) SEM (magnification of 35,000×) micrographs of drug-free, WGA-conjugated PLGA nanoparticles.

profiles were concentration- and time-dependent, with cellular uptake increasing with nanoparticle loading concentration and exposure time. Cell-associated fWN in the Caco-2 cells was doubled when the incubation time was prolonged from 0.5 to 3 h at the nanoparticle loading concentration of 1.25 mg/ml. An 8-fold increase in nanoparticle loading concentration resulted in 9.1-, 5.2- and 4.8-folds increase in the 2h-fWN uptake by the Caco-2, HT-29 and CCD-18Co cells, respectively. At all time points and loading concentrations studied, the ranking order of uptake was Caco-2 > HT-29 > CCD-18Co, suggesting a selectivity of the delivery system for colon cancer cells over normal cells. This would be advantageous when the system is used to deliver an anticancer agent to the colon tissues. Corresponding cellular uptakes of fBN are shown in Fig. 3(b), and these were lower in capacity compared with fWN uptakes in all three cell types. In the case of Caco-2 cells exposed to 1.25 mg/ml of nanoparticles, the fWN uptake after 3 h was about 12-folds higher than the fBN uptake.

3.4. Anti-proliferation activity of paclitaxel formulations

The paclitaxel formulations were evaluated for cytotoxic activity in the paclitaxel concentration range of 0.05–50 μg/ml. The highest drug concentration was equivalent to nanoparticle concentration of 1 mg/ml for the WNP and PNP formulations. At this concentration, the drug-free PLGA nanoparticles did not show any detectable cytotoxicity in that they did not reduce cell viability to below 80%.

The MTT assay suggested that the WNP, PNP and P/CreEL formulations yielded comparable paclitaxel IC_{50} values against the Caco-2 cells after 24 h co-incubation (Table 1). Enhanced cell-killing effects were observed for WNP, however, upon prolongation of the incubation time to 72 h, whereupon the IC_{50} value was significantly reduced to 0.087 ± 0.020 μg/ml. The IC_{50} value of WNP was 2.6 and 4.1-folds lower than those of PNP and P/CreEL, respectively, for Caco-2 cells at 72 h.

IC_{50} values against the HT-29 cells were generally lower than those against the Caco-2 cells, suggesting that the HT-29 cells were more sensitive to paclitaxel. For this cell line, significant differences in efficacy were observed between the nanoparticle formulations, WNP and PNP, and the conventional P/CreEL formulation even at the shorter incubation time of 24 h. There were also statistical differences between the IC_{50} values for WNP and PNP (Table 1) at both 24 and 72 h of incubation. When the incubation time was extended to 72 h, enhanced cell-killing effects were observed for WNP, which showed a significantly reduced IC_{50} value of 0.028 ± 0.008. This value was statistically different to the IC_{50} of P/CreEL at 72 h incubation.

For all cell types, the ranking order of efficacy of the three paclitaxel formulations was WNP > PNP > P/CreEL at both 24 h and 72 h. The prolongation of incubation time produced increased discrepancy among the IC_{50} value of the formulations. The CCD-18Co cells showed no difference in sensitivity towards WNP compared to PNP. However, both the WNP and the PNP had lower IC_{50} values compared to conventional P/CreEL formulation towards CCD-18Co cells.

3.5. Cellular accumulation and efflux of paclitaxel

Fig. 4 shows the data obtained for the cellular accumulation and retention of paclitaxel in the Caco-2, HT-29 and CCD-18Co cells exposed to the WNP, PNP and P/CreEL formulations. After 2 h of incubation, the cellular uptake of WNP was about 1.5- and 2-folds greater than that of PNP in the Caco-2 and HT-29 cells, respectively. WNP also demonstrated increased intracellular retention (30% of uptake) in the Caco-2 cells, following post-uptake incubation with fresh medium, compared to the unconjugated PNP nanoparticles (18%) and P/CreEL (7%). Similar phenomena were observed in the HT-29 cells, which retained more than 40% of the internalized WNP and 27% of PNP. The CCD-18Co cells, on the other hand, showed similar uptake and post-uptake reten-

Table 1
IC_{50} values of paclitaxel formulated as WNP, PNP and P/CreEL. IC_{50} values were evaluated after 24 and 72 h exposure and the results represent mean ± SD values (μg/ml) of three independent experiments, each performed in triplicate.

Sample	Incubation time (h)	Cell type		
		Caco-2	HT-29	CCD-18Co
WNP	24	1.019 ± 0.233	0.061 ± 0.021*	1.007 ± 0.121*
	72	0.087 ± 0.020*,^	0.028 ± 0.008*,^	0.137 ± 0.027*
PNP	24	1.141 ± 0.341	0.092 ± 0.030*	1.188 ± 0.170
	72	0.228 ± 0.031*,^	0.062 ± 0.015*	0.147 ± 0.035*
P/CreEL	24	1.387 ± 0.158	0.310 ± 0.019	1.665 ± 0.251
	72	0.355 ± 0.015	0.069 ± 0.013	0.230 ± 0.021

* Statistical significance compared to P/CreEL ($p < 0.05$).
^ Statistical significance between WNP and PNP formulations ($p < 0.05$).

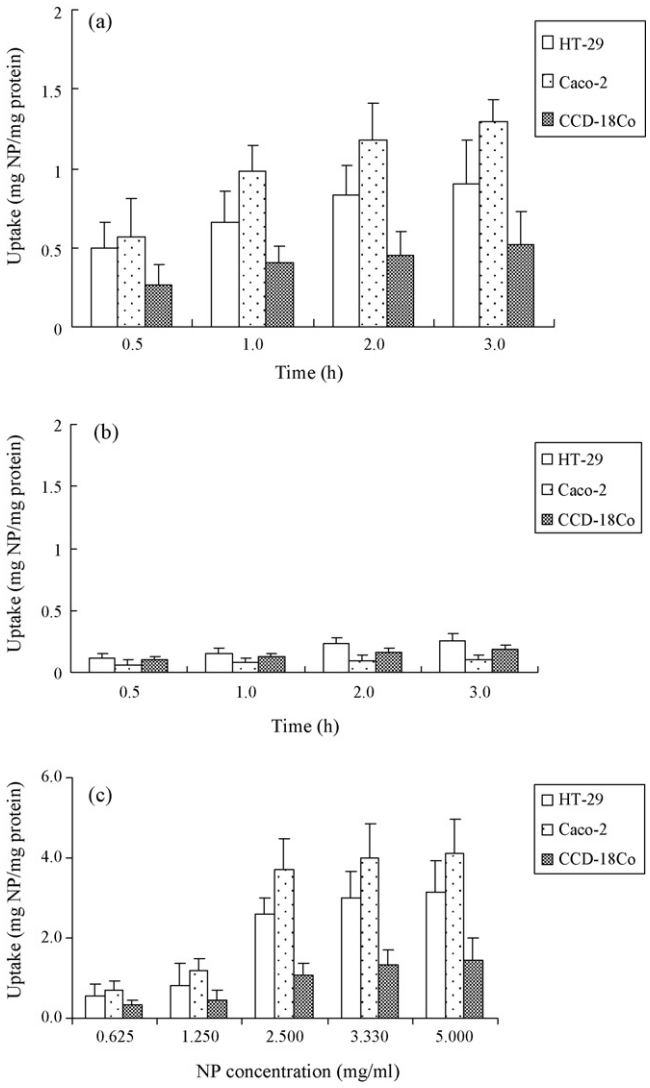

Fig. 3. Uptake of nanoparticles by the Caco-2, HT-29 and CCD-18Co cells (mean ± SD, $n = 3$). (a) Effect of fWN incubation time at the loading concentration of 1.25 mg/ml; (b) effect of fBN incubation time at the loading concentration of 1.25 mg/ml; (c) effect of fWN loading concentration on the 2-h cellular uptake.

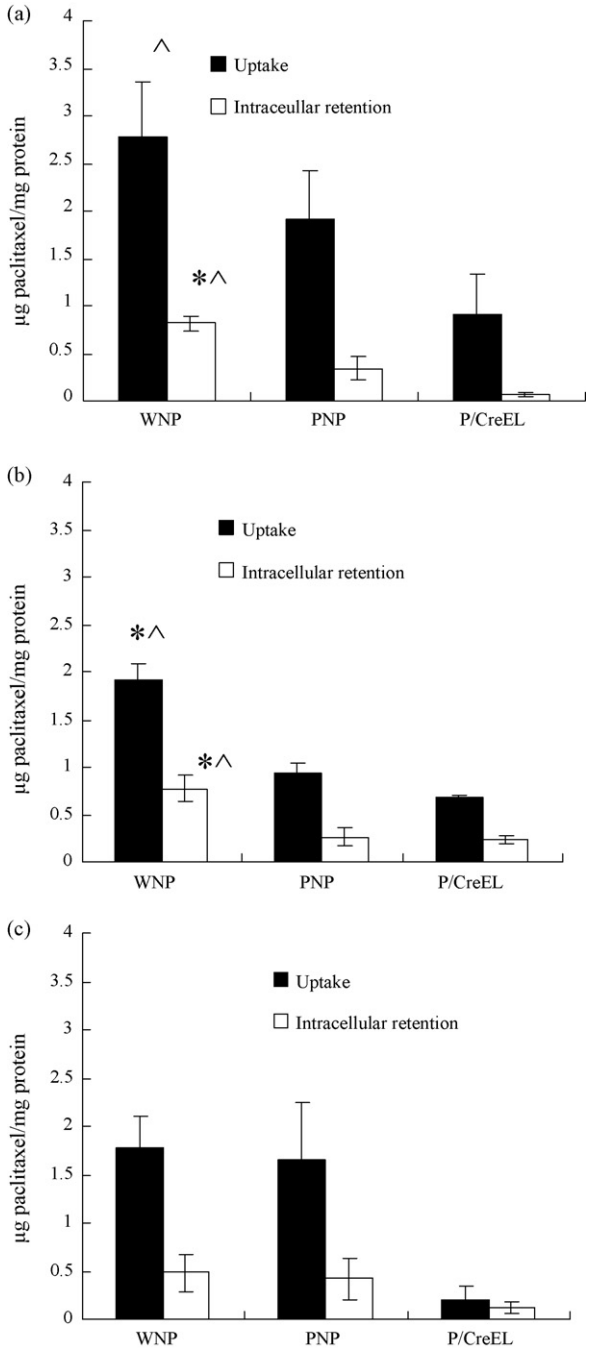

Fig. 4. Cellular uptake of paclitaxel after 2 h exposure to the WNP, PNP and P/CreEL formulations, and the intracellular retention of paclitaxel following post-uptake incubation of the cells with fresh medium; (a) Caco-2; (b) HT-29; (c) CCD-18Co cells. Data represent mean ± SD, $n = 3$. *Statistical significance between WNP and PNP, ^Statistical significance between WNP and P/CreEL ($p < 0.05$).

tion profiles of paclitaxel when exposed to the WNP and PNP formulations.

The Caco-2 and HT-29 cells exhibited an uptake and post-uptake retention preference that ranked in the order of WNP > PNP > P/CreEL. In contrast, the normal CCD-18Co colon cells did not show a clear preference for WNP uptake. The Caco-2 and HT-29 cells also retained more paclitaxel from the WNP formulation compared to the CCD-18Co cells. These results suggest that the formulation of paclitaxel into WGA-conjugated nanoparticles did not only enhance paclitaxel uptake but also resulted in higher drug retention by the cancerous colon cells.

3.6. Visualization of cell-associated nanoparticles

To differentiate between extracellular and internalized WNP, we repeated the uptake experiments on the three cell lines using a WNP formulation prepared with fWGA. The cells were incubated with the fWNP formulation for 1 h. The cells were incubated post-uptake with trypan blue so that any fluorescence attributed to extracellular fWNP might be quenched. Confocal microscopic images of the Caco-2, HT-29 and CCD-18Co cells (Fig. 5) show there were no significant changes in the cell-associated fluorescence after post-uptake TB incubation. A measurement of the cell lysate fluorescence for the Caco-2 cells before and after TB treatment indicated that 96.3% of the initial fWNP load was retained in the cells. The implication was that the cell-associated fWNP nanoparticles were located inside the cells and not on the cell surface.

3.7. Cellular trafficking of WGA-conjugated PLGA nanoparticles

Confocal microscopic analysis of Caco-2 cells incubated with fWNP demonstrated the uptake of the nanoparticles into the

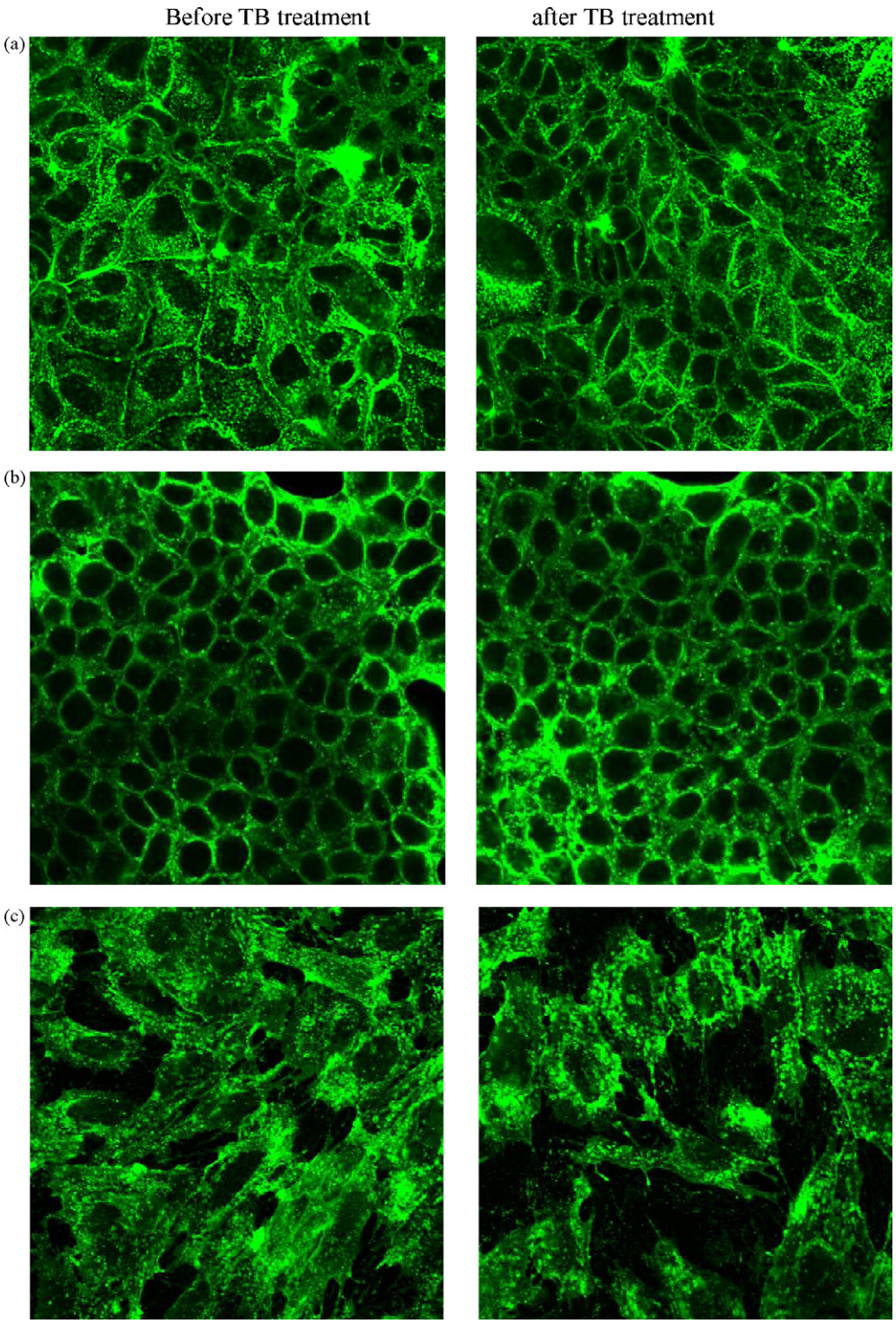

Fig. 5. Confocal images of (a) Caco-2; (b) HT-29; (c) CCD-18Co cells incubated with 1.0 mg/ml of fluorescent WNP for 1 h before and after trypan blue (TB) treatment.

intracellular space (Fig. 6). We stained the acidic compartments (endo-lysosomes) and nucleus of the cell with Lysosensor DND-99 (red) and Hoechst 33258 (blue), respectively, so that the co-localization of endo-lysosomes (red) and WNP (green) may be represented by yellow clusters. However, the yellow clusters were visible only if the red and green intensities are close to each other, thus limiting the interpretation of cellular events from visual inspection alone. To provide a quantitative estimate of the degree of co-localization of WNP and endo-lysosomes, the confocal images were processed with the program ImageJ (National Institutes of Health Bethesda, MD, USA). Data represent mean values calculated from the Z-series images of cells sequentially obtained by confocal laser scanning microscopy (Table 2). This method was preferred to the use of a single confocal image, which represented only a thin slice of the whole cells, and might not be representative of the true distribution of endo-lysosomal compartment and nanoparticles in the whole cell.

The data show that fWNP was internalized rapidly and could be detected inside the cells after 30 min incubation, both in the endo-lysosomes (yellow) and the cytoplasm (green). The intensity

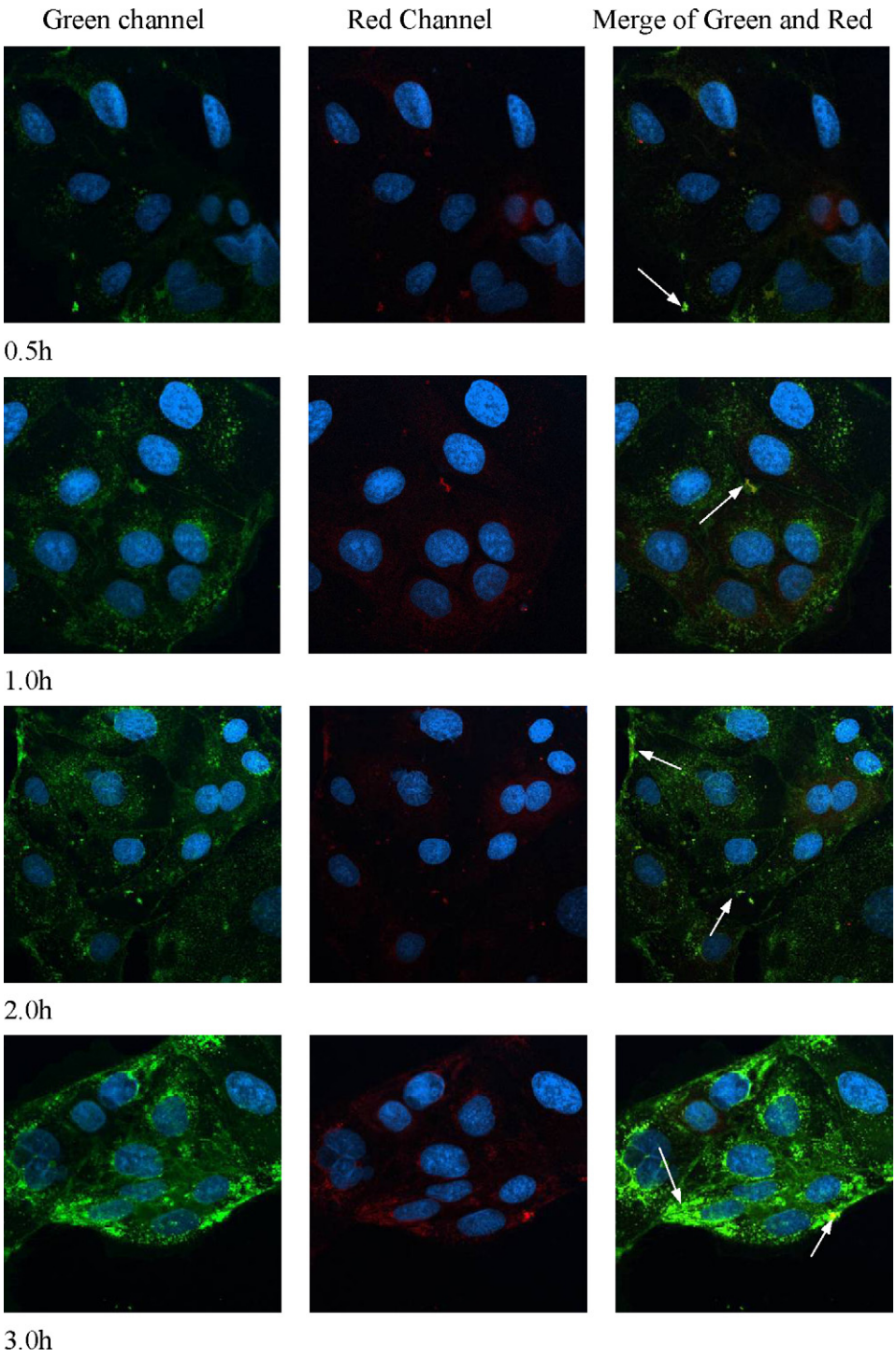

Fig. 6. Typical images of Caco-2 cells showing the intracellular trafficking of WNP following incubation of the cells with the formulation for various time periods. WNP nanoparticle has green fluorescence, cell nucleus is blue, and the overlap of nanoparticle and lysotracker® fluorescence (red) is shown as yellow (white arrows indicate). (For interpretation of the references to color in this figure legend, the reader is referred to the web version of the article.)

of green fluorescence in the cytoplasm increased with incubation time, which correlated with the increasing amount of internalized fWNP with time. The containment of the internalized fWNP in the late endo-lysosomal compartments also increased with incubation time, with 33% of the internalized fWNP estimated to be co-localized with the acidic compartments at 1 h, and almost 54% in 3 h. Nevertheless, the green fluorescence in the cytoplasm suggests that endocytosed fWNP was successfully released from the endo-lysosome into the cytoplasm. This release and the subsequent dissociation of paclitaxel from the fWNP nanoparticles would be imperative for the drug to exert its pharmacological action through binding with the cellular tubulin.

When the Caco-2 cells were pre-treated with unlabelled WGA prior to exposure to fWNP, the uptake of fWNP was greatly reduced. Fig. 7 shows a typical confocal image of the cells taken after 3 h incubation with fWNP. The significant absence of green fluorescence in these cells indicated a poor uptake of fWNP. The inhibition of fWNP uptake by pre-incubation with unlabelled WGA suggests the fWNP

Table 2
Co-localization of FITC-WNP (green) and endosome/lysosome (red) in Caco-2 cells determined as the percentage of voxels which had both red and green intensities above threshold, expressed as a percentage of the total number of pixels in the image.

Time (h)	Co-localization (yellow) (%)	Green in red (%)	Red in green (%)
0.5	11.29	32.75	33.56
1	12.75	32.02	29.15
2	13.96	43.80	34.52
3	25.42	53.99	44.90

uptake involved the specific interaction of WGA with its binding receptor in the Caco-2 cells.

4. Discussion

In order to use WGA as a tumor-targeting ligand, there is a need to establish the expression profile of its receptor glycoproteins in target cells. In this study, lectin blot analysis confirmed the differential expression levels of N-acetyl-D-glucosamine-containing glycoproteins in the cell membrane and intracellular compartments of Caco-2, HT-29 and CCD-18Co cells. The ranking order of expression of these glycoproteins suggests that normal colon cells may express lower levels of WGA-recognizable glycoproteins than the cancerous colon cells. The cellular glycoprotein expression was in agreement with the higher agglutination selectivity of fWGA for the Caco-2 and HT-29 cells relative to the CCD-18Co cells.

In vitro anti-proliferation activity of WNP, PNP and P/CreEL confirmed that WGA conjugation enhanced the cytotoxicity of the paclitaxel-loaded PLGA nanoparticles against the colon cancer cells. In line with its glycoprotein expression level and its greater susceptibility to paclitaxel, as indicated by the P/CreEL data, the HT-29 cells were more sensitive than the Caco-2 cells to the effects of WNP. WNP was also significantly more cytotoxic towards the Caco-2 cells than the CCD-18Co cells at 72 h, in keeping with the uptake data. This indicated that the higher cytotoxicity observed for WNP was a result of enhanced intracellular paclitaxel concentration. In contrast, the PNP and P/CreEL formulations did not show differential cytotoxicities against the cancer and normal cells at 72 h, and the IC_{50} for WNP against the Caco-2 and HT-29 cells were, respectively, 1.6- and 4.9-folds lower than those of P/CreEL after 72 h incubation.

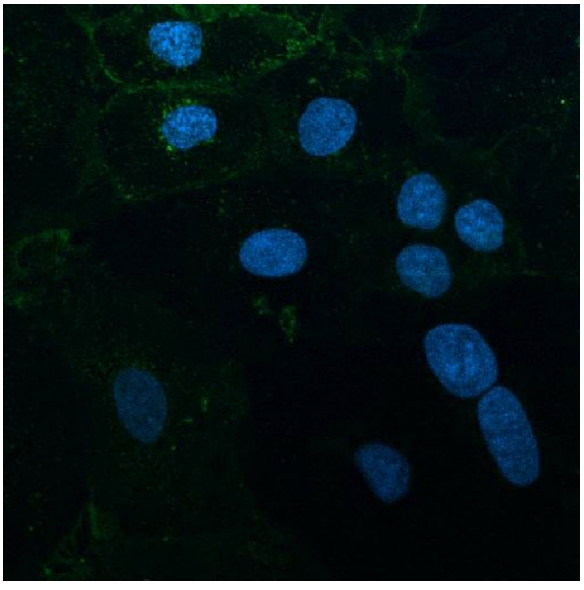

Fig. 7. Typical confocal image of Caco-2 cells pre-treated with unlabelled WGA and then incubated with fWNP for 3 h.

On this basis, the WNP could be considered a superior paclitaxel formulation compared to PNP and P/CreEL.

WNP showed time-dependent paclitaxel IC_{50} values for all three colon cell types, indicating a prolonged incubation time was required to raise the intracellular drug concentration to therapeutic level. This time lag could be required for the drug to be released from the nanoparticles in the cell cytoplasm. Nevertheless, the paclitaxel IC_{50} values attained with the WNP formulation were consistently lower than those obtained with the P/CreEL and PNP formulations tested under similar conditions. A comparison of IC_{50} values for WNP suggests that its anti-proliferative activity against HT-29 was weaker than that against A549, a representative lung cancer cell model (Mo and Lim, 2005a). In addition, WNP exhibited time-independent IC_{50} values against the A549 cells (Mo and Lim, 2005a,b). The different cellular responses might be due to inherent differences in cellular glycoprotein expression or sensitivity towards paclitaxel, as exemplified by data derived with the Caco-2 and HT-29 cells in this study.

The greater efficacy of WNP in the colon cancer cells correlated well with the higher cellular uptake and sustained intracellular retention of paclitaxel associated with the formulation. Cellular uptake was facilitated by the over-expression of N-acetyl-D-glucosamine-containing glycoprotein on the colon cell surface, as the uptake mechanism was readily inhibited by the presence of unlabelled WGA, suggesting WGA-mediated receptor interaction. The measurement of cellular fluorescence post-TB incubation suggested that most of the cell-associated WNP was located intracellularly, in line with other studies that demonstrated an enhanced cellular uptake of drug and drug delivery systems following WGA conjugation (Gabor et al., 2004; Mo and Lim, 2005a). On the other hand, the effect of WGA conjugation on intracellular drug retention has not been investigated. Our results showed that WGA-conjugated PLGA nanoparticles could indeed increase the retention of paclitaxel inside the colon cancer cells, and this was likely promoted by the binding of the conjugated WGA to the glycoproteins expressed on the cytoplasmic side of the cell membrane. Therefore, the advantages of WNP vis-à-vis P/CreEL are multiple fold when the enhanced cellular uptake, intracellular drug retention and sustainable drug release features were considered.

Insight into the intracellular translocation of WNP is important in providing a measure of its effectiveness as an anticancer drug delivery system. Following endocytic uptake, nanoparticles may be transferred into early sorting endosomes and recycling endosomes or transferred from early endosomes to late endosomes–lysosomes (Vasir and Labhasetwar, 2008). Our study showed about 30% of the endocytosed WNP to be present in the late endo-lysosomes, with fluorescence measurements suggesting increasing amount of internalized WNP with time. Subsequent increase in cytosolic fluorescence, indicative of the successful escape of the WNP from the endo-lysosome compartment into the cytosol, might be explained by a reversal (from anionic to cationic) of the negative charge on the WNP nanoparticle surface when confronted with the acidic pH in the endo-lysosomes compartment (Panyam et al., 2002). The progression of events from cell entry to eventual drug release from the nanoparticles would account for why cell damage/death occurred only after prolonged incubation when WNP was internalized at a rapid rate into the colon cells.

5. Conclusion

WNP had superior *in vitro* anti-proliferation activity against the colon cancer cell lines, Caco-2 and HT-29, compared with the PNP and P/CreEL formulations. It was, however, less toxic against the normal colon fibroblast, CCD-18Co cells, than against the cancer cell lines. The enhanced cytotoxicity of WNP in the colon cancer

cells could be attributed to a more efficient cellular internalization of paclitaxel via WGA-mediated endocytosis, and a more efficient retention of the drug within the cells. The anti-cytoproliferation activity of WNP was dependent on incubation time and loading concentration. Co-localization studies indicated that the endocytosed WNP could escape from the endo-lysosomal compartment into the cytosol.

References

Andreopoulou, E., Muggia, F., 2008. Pharmacodynamics of tubulin and tubulin-binding agents: extending their potential beyond taxanes. Clin. Breast Cancer 8, S54–S60.

Boland, C.R., Montgomery, C.K., Kim, Y.S., 1982. Alterations in human colonic mucin occurring with cellular differentiation and malignant transformation. Proc. Natl. Acad. Sci. U.S.A. 79, 2051–2055.

Caldero, J., Campo, E., Ascaso, C., Ramos, J., Panades, M.J., Rene, J.M., 1989. Regional distribution of glycoconjugates in normal, transitional and neoplastic human colonic mucosa – a histochemical-study using lectins. Virchows Arch. A – Pathol. Anat. Histopathol. 415, 347–356.

Campo, E., Condom, E., Palacin, A., Quesada, E., Cardesa, A., 1988a. Lectin binding patterns in normal and neoplastic colonic mucosa – a study of Dolichos-biflorus agglutinin, peanut agglutinin, and wheat-germ agglutinin. Dis. Colon Rectum 31, 892–899.

Campo, E., Condom, E., Palacin, A., Quesada, E., Cardesa, A., 1988b. Lectin binding patterns in normal and neoplastic colonic mucosa. A study of Dolichos biflorus agglutinin, peanut agglutinin, and wheat germ agglutinin. Dis. Colon Rectum 31, 892–899.

Casadei, M.A., Pitarresi, G., Calabrese, R., Paolicelli, P., Giammona, G., 2008. Biodegradable and pH-sensitive hydrogels for potential colon-specific drug delivery: characterization and in vitro release studies. Biomacromolecules 9, 43–49.

Chen, H.M., Langer, R., 1998. Oral particulate delivery: status and future trends. Adv. Drug Deliv. Rev. 34, 339–350.

Chen, H.W., Gao, J., Lu, Y., Kou, G., Zhang, H., Fan, L., Sun, Z.G., Guo, Y.J., Zhong, Y.Q., 2008. Preparation and characterization of PE38KDEL-loaded anti-HER2 nanoparticles for targeted cancer therapy. J. Control. Release 128, 209–216.

De Dosso, S., Sessa, C., Saletti, P., 2009. Adjuvant therapy for colon cancer: present and perspectives. Cancer Treat. Rev. 35, 160–166.

Gabor, F., Bogner, E., Weissenboeck, A., Wirth, M., 2004. The lectin–cell interaction and its implications to intestinal lectin-mediated drug delivery. Adv. Drug Deliv. Rev. 56, 459–480.

Gabor, F., Stangl, M., Wirth, M., 1998. Lectin-mediated bioadhesion: binding characteristics of plant lectins on the enterocyte-like cell lines Caco-2, HT-29 and HCT-8. J. Control. Release 55, 131–142.

Heinrich, E.L., Welty, L.A.Y., Banner, L.R., Oppenheimer, S.B., 2005. Direct targeting of cancer cells: a multiparameter approach. Acta Histochem. 107, 335–344.

Holt, P.R., Kozuch, P., Mewar, S., 2009. Colon cancer and the elderly: from screening to treatment in management of GI disease in the elderly. Best Pract. Res. Clin. Gastroenterol. 23, 889–907.

Huh, J.W., Park, Y.A., Lee, K.Y., Sohn, S.K., 2009. Heterogeneity of adenosine triphosphate-based chemotherapy response assay in colorectal cancer – secondary publication. Yonsei Med. J. 50, 697–703.

Jang, S.H., Wientjes, M.G., Lu, D., Au, J.L.S., 2003. Drug delivery and transport to solid tumors. Pharm. Res. 20, 1337–1350.

Keegan, M.E., Royce, S.M., Fahmy, T., Saltzman, W.M., 2006. In vitro evaluation of biodegradable microspheres with surface-bound ligands. J. Control. Release 110, 574–580.

Kim, G., Nie, S., 2005. Targeted cancer nanotherapy. Mater. Today 8, 28–33.

Lehr, C.M., 2000. Lectin-mediated drug delivery: the second generation of bioadhesives. J. Control. Release 65, 19–29.

Minko, T., 2004. Drug targeting to the colon with lectins and neoglycoconjugates. Adv. Drug Deliv. Rev. 56, 491–509.

Mo, Y., Lim, L.Y., 2005a. Paclitaxel-loaded PLGA nanoparticles: potentiation of anticancer activity by surface conjugation with wheat germ agglutinin. J. Control. Release 108, 244–262.

Mo, Y., Lim, L.Y., 2005b. Preparation and in vitro anticancer activity of wheat germ agglutinin (WGA)-conjugated PLGA nanoparticles loaded with paclitaxel and isopropyl myristate. J. Control. Release 107, 30–42.

Mohamed, F., van der Walle, C.F., 2008. Engineering biodegradable polyester particles with specific drug targeting and drug release properties. J. Pharm. Sci. 97, 71–87.

Panyam, J., Labhasetwar, V., 2003. Biodegradable nanoparticles for drug and gene delivery to cells and tissue. Adv. Drug Deliv. Rev. 55, 329–347.

Panyam, J., Zhou, W.Z., Prabha, S., Sahoo, S.K., Labhasetwar, V., 2002. Rapid endo-lysosomal escape of poly(DL-lactide-co-glycolide) nanoparticles: implications for drug and gene delivery. FASEB J. 16, 10.

Parveen, S., Sahoo, S.K., 2008. Polymeric nanoparticles for cancer therapy. J. Drug Target. 16, 108–123.

Patel, M., Shah, T., Amin, A., 2007. Therapeutic opportunities in colon-specific drug-delivery systems. Crit. Rev. Ther. Drug Carrier Syst. 24, 147–202.

Plattner, V.E., Ratzinger, G., Engleder, E.T., Gallauner, S., Gabor, F., Wirth, M., 2009. Alteration of the glycosylation pattern of monocytic THP-1 cells upon differentiation and its impact on lectin-mediated drug delivery. Eur. J. Pharm. Biopharm. 73, 324–330.

Pusztai, A., Ewen, S.W.B., Grant, G., Brown, D.S., Stewart, J.C., Peumans, W.J., Vandamme, E.J.M., Bardocz, S., 1993. Antinutritive effects of wheat-germ agglutinin and other N-acetylglucosamine-specific lectins. Br. J. Nutr. 70, 313–321.

Sahlin, S., Hed, J., Rundquist, I., 1983. Differentiation between attached and ingested immune-complexes by a fluorescence quenching cytofluorometric assay. J. Immunol. Methods 60, 115–124.

Sahoo, S.K., Labhasetwar, V., 2003. Nanotech approaches to delivery and imaging drug. Drug Discov. Today 8, 1112–1120.

Singla, A.K., Garg, A., Aggarwal, D., 2002. Paclitaxel and its formulations. Int. J. Pharm. 235, 179–192.

Suffness, M., Wall, M.E., 1995. Taxol®: Science and Applications. CRC Press, Boca Raton, FL.

Thiele, L., Rothen-Rutishauser, B., Jilek, S., Wunderli-Allenspach, H., Merkle, H.P., Walter, E., 2001. Evaluation of particle uptake in human blood monocyte-derived cells in vitro. Does phagocytosis activity of dendritic cells measure up with macrophages? J. Control. Release 76, 59–71.

Trissel, L.A., 1996. Pharmaceutical Properties of Paclitaxel and their Effects on Preparation and Administration. University-of-Maryland-Cancer-Center Conference on Antineoplastics, San Francisco, CA, pp. S133–S139.

Trissel, L.A., Xu, Q.Y., Kwan, J., Martinez, J.F., 1994. Compatibility of paclitaxel injection vehicle with intravenous administration and extension sets. Am. J. Hosp. Pharm. 51, 2804–2810.

van Vlerken, L.E., Duan, Z.F., Seiden, M.V., Amiji, M.M., 2007. Modulation of intracellular ceramide using polymeric nanoparticles to overcome multidrug resistance in cancer. Cancer Res. 67, 4843–4850.

Vasir, J.K., Labhasetwar, V., 2008. Quantification of the force of nanoparticle-cell membrane interactions and its influence on intracellular trafficking of nanoparticles. Biomaterials 29, 4244–4252.

Yang, L., 2008. Biorelevant dissolution testing of colon-specific delivery systems activated by colonic microflora. J. Control. Release 125, 77–86.

Zhan, M., Tao, W.Y., Pan, S.H., Sun, X.Y., Jiang, H.C., 2009. Low-dose metronomic chemotherapy of paclitaxel synergizes with cetuximab to suppress human colon cancer xenografts. Anti-Cancer Drug. 20, 355–363.